Published in final edited form as:
J Immunol. 2008 October 15; 181(8): 5433–5441.

Endoplasmic Reticulum Stress Regulator XBP-1 Contributes to Effector CD8+ T Cell Differentiation during Acute Infection[1]

Daisuke Kamimura and **Michael J. Bevan**[2]
Department of Immunology and Howard Hughes Medical Institute, University of Washington, Seattle, WA 98195

Abstract

The transcription factor X-box-binding protein-1 (XBP-1) plays an essential role in activating the unfolded protein response in the endoplasmic reticulum (ER). Transcribed XBP-1 mRNA is converted to its active form by unconventional cytoplasmic splicing mediated by inositol-requiring enzyme-1 (IRE-1) upon ER stress. We report activation of the IRE-1/XBP-1 pathway in effector $CD8^+$ T cells during the response to acute infection. Transcription of unspliced XBP-1 mRNA is up-regulated by IL-2 signals, while its splicing is induced after TCR ligation. Splicing of XBP-1 mRNA was evident during the expansion of Ag-specific $CD8^+$ T cells in response to viral or bacterial infection. An XBP-1 splicing reporter revealed that splicing activity was enriched in terminal effector cells expressing high levels of killer cell lectin-like receptor G1 (KLRG1). Overexpression of the spliced form of XBP-1 in $CD8^+$ T cells enhanced KLRG1 expression during infection, whereas XBP-$1^{-/-}$ $CD8^+$ T cells or cells expressing a dominant-negative form of XBP-1 showed a decreased proportion of $KLRG1^{high}$ effector cells. These results suggest that, in the response to pathogen, activation of ER stress sensors and XBP-1 splicing contribute to the differentiation of end-stage effector $CD8^+$ T cells.

The $CD8^+$ T cell response to acute infection entails vigorous expansion of Ag-specific cells, generating effector cells that are able to secrete various cytokines and cytotoxic molecules. Following acute infection, naive Ag-specific $CD8^+$ T cells may divide more than 14 times within 1 wk and acquire effector functions that contribute to eradication of the pathogen (1). Although most effector cells undergo programmed cell death when the infection is controlled, a small number are left behind and maintained as long-lived memory cells (2). Although the mechanisms underlying this cell fate decision are still debated, cell surface markers distinguishing these subsets have been identified. Following down-regulation of CD127 expression on activation, effector $CD8^+$ T cells that regain high level CD127 expression preferentially give rise to memory cells (3). In addition, recent studies demonstrated that surface expression levels of the killer cell lectin-like receptor G1 (KLRG1)[3] molecule on effector $CD8^+$ T cells also report this cell fate decision. Terminally differentiated or end-stage effector cells are $KLRG1^{high}$, whereas memory precursor effector cells are $KLRG1^{low}$ (4,5).

---

[1]This work was supported by the Howard Hughes Medical Institute and by Grant AI19335 from the National Institutes of Health (to M.J.B.).

2Address correspondence and reprint requests to Dr. Michael J. Bevan, Department of Immunology, Office I604H Health Science Center, Box 357370, University of Washington, 1959 NE Pacific Street, Seattle, WA 98195-7370. mbevan@u.washington.edu.

Disclosures
The authors have no financial conflict of interest.

[3]Abbreviations used in this paper: KLRG1, killer cell lectin-like receptor G1; ER, endoplasmic reticulum; ERAI, ER stress-activated indicator; ATF, activating transcription factor; eIF2α, eukaryotic translation initiation factor 2α; IRE-1, inositol-requiring enzyme-1; XBP-1, X-box-binding protein-1; LCMV, lymphocytic chorio-meningitis virus; PERK, protein kinase R-like ER kinase; p.i., postinfection; UPR, unfolded protein response; WT, wild type.

This recent work also showed that inflammatory cytokines or prolonged antigenic stimulation favor differentiation of the KLRG1^{high} end-stage effector population characterized by less homeostatic turnover and lower IL-2 production (4,5).

Among many cytokines that constitute inflammatory environments, a number of groups have reported that IL-2 plays a critical role in CD8$^+$ T cell responses to infection. For example, IL-2 injection during viral infection differentially affects CD8$^+$ T cell responses, depending on the timing of the treatment (6). In addition, CD8$^+$ T cells lacking CD25, a component of the high-affinity IL-2R, expand severalfold less and form a greater proportion of CD62L^{high} central memory phenotype cells than do wild-type (WT) cells (7–9). In addition, CD25$^{-/-}$ memory CD8$^+$ cells are normally maintained, but are incapable of robust recall responses (8,9). Treatment of mice with IL-2/anti-IL-2 mAb complexes (IL-2 complex) is a useful way to deliver IL-2 signals in vivo (10,11). Following IL-2 complex treatment, naive CD8$^+$ T cells differentiate into effector and memory-like cells without exogenous Ag stimulation (12). These observations indicate a diverse regulatory role for IL-2 signals, driving cells to full effector and memory differentiation, and led us to look for IL-2 target genes that affect CD8$^+$ T cell responses.

ER stress caused by the accumulation of unfolded proteins in the ER activates the unfolded protein response (UPR), a mechanism that restores homeostasis in the ER. This response includes up-regulation of ER chaperones and of proteins involved in ER-associated protein degradation. Many factors are known to cause ER stress, including massive synthesis of secretory proteins, changes in calcium concentration, imbalance of the redox state, and nutrient deprivation (13–15). There are three major sensors of ER stress that trigger UPR, namely the pathways using the factors inositol-requiring enzyme-1 (IRE-1) and X-box-binding protein-1 (XBP-1) (IRE-1/XBP-1), activating transcription factor (ATF)6, and protein kinase R-like ER kinase (PERK) and eukaryotic translation initiation factor 2α subunit (eIF2α) (PERK/eIF2α) (13–15). XBP-1 is a basic leucine zipper family transcription factor, the activity of which is uniquely regulated by an unconventional cytoplasmic splicing reaction mediated by IRE-1, an ER resident kinase/RNase. XBP-1 mRNA is synthesized as a precursor form with an extra intron of 26 nucleotides (16,17). This unspliced form of mRNA (XBP-1u) has an open reading frame containing a DNA binding domain in the N terminus, and a degradation motif and nuclear exclusion signal in the C terminus (18). Upon ER stress, IRE-1 is activated and splices out the 26-nt intron, causing a frame shift of the coding region of XBP-1. The resulting spliced form (XBP-1s) encodes a longer polypeptide that retains the DNA binding domain, with a newly generated transactivating domain in the C terminus (16,17). Microarray analyses using XBP1$^{-/-}$ embryonic fibroblasts under ER stress revealed several XBP-1-dependent UPR target genes including ERdj4, P58^{IPK}, EDEM, RAMP-4, PDI-P5, and HEDJ (19). In addition to genes involved in UPR, XBP-1 binds to a diverse set of genes in a cell type- and condition-specific manner (20). In vitro studies have shown that cells that have adapted to chronic ER stress by activating UPR become more resistant to subsequent stress, whereas those that have failed to adapt undergo apoptosis (21). When IRE-1 activity was artificially sustained in human cell lines, cell survival was enhanced upon ER stress in vitro (22), suggesting that the IRE-1/XBP-1 axis affects the cell fate decision between cell death and survival.

XBP-1$^{-/-}$ mice die before birth from anemia associated with hypoplasia in the fetal liver (23). Hepatocyte-specific transgenic expression of XBP-1 rescues the embryonic lethality of XBP-1$^{-/-}$ mice, but these animals display abnormalities in other secretory organs such as the pancreas, leading to neonatal death (24). In the immune system, RAG2$^{-/-}$ blastocyst complementation revealed an essential role for XBP-1 in the generation of plasma cells. XBP-1$^{-/-}$ B cells develop normally, undergo class-switch recombination, and form germinal centers upon activation, but they fail to secrete Igs (25). In B cells, transcription of XBP-1u mRNA is directly up-regulated by IL-4 signaling, but splicing to XBP-1s is dependent on

additional signals that induce synthesis of Igs during differentiation into plasma cells (26). Surprisingly, it has recently been shown that XBP-1 is also important for the development and survival of dendritic cells that are not known to be highly secretory (27).

In this study, we identified XBP-1 as an IL-2-induced gene in $CD8^+$ T cells in vivo, and demonstrate the activation of the IRE-1/XBP-1 splicing machinery in effector $CD8^+$ T cells during acute infection.

Materials and Methods

Mice

C57BL/6J mice were obtained from The Jackson Laboratory. OVA-specific OT-I TCR transgenic mice on the $RAG1^{-/-}$ background (OT-I/$RAG1^{-/-}$) were purchased from Taconic Farms. XBP-1/$RAG2^{-/-}$ blastocyst chimeras (25) and 129/$RAG2^{-/-}$ control chimeras were provided by L. Glimcher (Harvard School of Public Health, Boston, MA). These blastocyst chimeras were used for generation of secondary bone marrow chimeric mice using 10 Gy-irradiated C57BL/6J mice as hosts. XBP-$1^{-/-}$ $CD8^+$ T cells (129 strain origin) were detected by the CD229.1 marker (30C7; BD Biosciences). ERAI transgenic mice (28) were obtained from the RIKEN BioResource Center (Ibaraki, Japan) with the kind approval of M. Miura (Graduate School of Pharmaceutical Sciences, University of Tokyo, Tokyo, Japan). Animals were housed in specific pathogen-free conditions in the animal facilities at the University of Washington. P14 TCR transgenic mice specific for lymphocytic choriomeningitis virus (LCMV) $gp_{33–41}$ and OT-I mice congenic for Thy1.1 or CD45.1 were bred and maintained in the same facilities. All experiments were performed in compliance with the University of Washington Institutional Animal Care and Use Committee regulations.

IL-2 complex treatment and DNA microarray analysis

IL-2/anti-IL-2 mAb complexes (IL-2 complex) were prepared and injected i.p. as previously described (12). After 1 and 3 h, total $CD8^+$ T cells were purified by magnetic cell sorting using the $CD8a^+$ T cell isolation kit (Miltenyi Biotec), supplemented with biotinylated anti-CD11c, anti-CD19, anti-Gr-1, anti-TCR $\gamma\delta$, anti-I-A^b, and anti-NK1.1 mAbs (BD Biosciences and eBioscience). $CD8^+$ T cells from nontreated mice served as a control (0 h). Total RNA from the purified $CD8^+$ T cells was subject to DNA microarray analysis using GeneChip Mouse genome 430 2.0 array (Affymetrix). Target labeling, hybridization, and scanning were performed at the Center for Array Technologies (University of Washington, Seattle, WA).

Bacterial and viral infection

Listeria monocytogenes expressing a secreted form of OVA (LM-OVA) (29) and *L. monocytogenes* secreting the LCMV gp_{33} epitope (LM-GP_{33}) were provided by H. Shen (University of Pennsylvania School of Medicine, Philadelphia, PA). LM-OVA and LM-GP_{33} were grown as previously described (12). LCMV was grown on BHK cells and was titrated on Vero cells. For bacteria infection, mice were injected i.v. with a priming dose of 3000 CFU, and a challenge dose of $1–2 \times 10^5$ CFU. For LCMV infection, a dose of 2×10^5 PFU was i.p. injected. Ampicillin treatment of *Listeria*-infected mice was performed as previously described (30).

Western blot analysis

$CD8^+$ T cells were stimulated for 2 days with 1 μg/ml each of anti-CD3 (145-2C11) and anti-CD28 (37.51) on a dish precoated with 300 μg/ml anti-hamster IgG (Jackson ImmunoResearch Laboratories), and then maintained in RPMI 1640 medium (Invitrogen) containing 10% FCS, antibiotics, and 100 U/ml mouse recombinant IL-2 (eBioscience). A few days later, these cells

were stimulated with plate-bound anti-CD3 and anti-CD28 mAbs for the indicated time periods. A proteasome inhibitor MG132 (Cal-biochem) was added to the culture at 1 μM for the last 1 h of the incubation to detect rapidly degraded XBP-1u protein (16,31). The sample at 0 h was cultured for 1 h with MG132. Total cell lysates equivalent to 2×10^6 cells were separated on SDS-PAGE, transferred to polyvinylidene difluoride membranes, and probed with anti-XBP-1 Ab (M-186; Santa Cruz Biotechnology). Donkey anti-rabbit IgG-HRP (GE Healthcare) was used as the secondary Ab, and signals were detected using the ECL western blotting detection kit (GE Healthcare).

RT-PCR and real-time PCR of XBP-1 mRNA

To distinguish XBP-1u and XBP-1s mRNAs, a region encompassing the splicing site of XBP-1 was amplified by RT-PCR with saturating cycles, followed by digestion with *Pst*I, whose recognition site is located within the 26-nt intron of XBP-1u mRNA (17). For real-time PCR, a primer set was designed to bind upstream of the splicing site to detect total XBP-1 transcripts, including both XBP-1u and XBP-1s mRNA in the same product size. Real-time PCR was performed using the SuperScript III Platinum Two-Step QRT-PCR kit with SYBR Green (Invitrogen). Mouse recombinant IL-2, IL-4, IL-6, and IL-12 and human recombinant IL-15 were obtained from BD Biosicences, eBioscience, and PeproTech.

Retroviral transduction of CD8$^+$ T cells

Retroviruses were produced using Phoenix-E cells transfected with pMit (MSCV-IRES-Thy1.1) vector (32), a gift from P. Marrack (National Jewish Medical and Research Center, Denver, CO). XBP-1u and XBP-1s cDNA were isolated by PCR using cDNA from a mouse melanoma cell line. To prevent IRE-1-mediated splicing of transduced XBP-1u, point mutations were introduced without amino acid substitutions at critical regions for the splicing (16). The XBP-1 splicing reporter construct, F-*XBP1*-ΔDBD-Venus, was a gift from M. Miura (Graduate School of Pharmaceutical Sciences, University of Tokyo, Tokyo, Japan) (28). GFP-RV vector (33) containing T-bet cDNA was provided by L. Glimcher (Harvard School of Public Health, Boston, MA). The dominant-negative form of XBP-1 was cloned as previously described (34). For retroviral transduction, OT-I/RAG1$^{-/-}$ cells were stimulated with plate-bound anti-CD3 and anti-CD28 mAbs, as described earlier. The activated OT-I/RAG1$^{-/-}$ cells were spin-infected twice with retroviruses on days 2 and 3 in the presence of 4 μg/ml polybrene (Sigma-Aldrich) and 100 U/ml IL-2, and maintained for 2–3 days in IL-2-containing medium until sorting. For Fig. 3*F*, transduced OT-I cells were obtained from bone marrow chimera mice that have been transplanted with retrovirus-infected OT-I bone marrow cells (35). Thy1.1$^+$ transduced cells were sorted using a FACSAria, and 10^4 cells/mouse were transferred i.v. into B6 mice. These animals were infected with LM-OVA on the same day or 1 day later.

Flow cytometry

Splenocytes and peripheral blood leukocytes were stained with fluorochrome-conjugated mAbs or $D^b gp_{33}$ tetramer complexed with streptavidin-PE in PBS containing 2% FCS and anti-CD16/CD32 mAb (2.4G2). Phospho-STAT5 staining was performed as described (12). For intracellular cytokine staining, splenocytes were incubated with 100 ng/ml $OVA_{257–264}$ or LCMV $gp_{33–41}$ peptides in the presence of brefeldin A (BD Biosciences, GolgiPlug) for 4 h at 37°C. After staining cell surface molecules, intracellular cytokine staining was performed using the Cytofix/Cytoperm kit (BD Biosciences). Fluorochrome-labeled mAbs were obtained from BD Biosciences, eBioscience, and BioLegend. Stained cells were analyzed on FACSCanto II (BD Biosciences), and data were processed by FlowJo software (Tree Star).

Statistical analysis

Statistical differences between groups were examined by a one-way ANOVA with Bonferroni's multiple comparison test or by an unpaired Student's *t* test using Prism software (GraphPad). A value of $p < 0.05$ was considered statistically significant.

Results

XBP-1 is an IL-2 target gene in CD8$^+$ T cells in vivo

To understand the mechanisms by which IL-2 signals control CD8$^+$ T cell responses, we conducted a genome-wide expression analysis. We used injection of IL-2 complex to deliver IL-2 signals to all CD8$^+$ T cells in vivo. Because STAT5 phosphorylation peaked 1 h after injection of the IL-2 complex (12) (Fig. 1*A*), gene expression in CD8$^+$ T cells was compared at 0 h (no treatment), 1 h, and 3 h posttreatment (Fig. 1*A*). Tables I and II show genes that were up-regulated and down-regulated more than 4-fold at 1 vs 0 h. A full list can be found in the Gene Expression Omnibus database (GSE11446). In the present study, we focused on XBP-1 because this transcription factor was found to be most up-regulated by IL-2 signals (Table I), and because XBP-1 is known to be critically involved in the differentiation and survival of immune cells, including plasma cells and dendritic cells (25,27). Real-time PCR confirmed the up-regulation of total XBP-1 transcripts in CD8$^+$ T cells after IL-2 complex treatment (Fig. 1*B*). XBP-1u and XBP-1s messages can be distinguished in size by RT-PCR combined with restriction enzyme digestion (17). Although IL-2 complex treatment increased the total amount of XBP-1 mRNA in CD8$^+$ T cells, it did not induce the conversion of XBP-1u to XBP-1s by 3 h (Fig. 1*C*), at which point, STAT5 phosphorylation and XBP-1 induction had already begun to fade (Fig. 1, *A* and *B*). IL-2 complex treatment in vivo activates STAT5 signaling in CD8$^+$ T cells as early as 15 min after treatment (12), suggesting the direct action of IL-2 signals on XBP-1 mRNA induction in CD8$^+$ T cells in vivo. In support of this idea, we found that in vitro stimulation with IL-2 up-regulated XBP-1 mRNA in purified CD8$^+$ T cell blasts (Fig. 1*D*), which formally excluded the possibility of a secondary effect of the complex through another cell type expressing the IL-2R. In addition to IL-2, IL-4 and IL-15 also increased total XBP-1 mRNA levels in CD8$^+$ T cells in vitro (Fig. 1*D*). These results demonstrate that IL-2 signals induce XBP-1u mRNA in CD8$^+$ T cells, but they do not generate the spliced, transcriptionally active form of XBP-1.

TCR ligation induces the generation of XBP-1s in vitro

We next tested whether TCR cross-linking induces the generation of XBP-1s. CD8$^+$ T cells were activated by plate-bound anti-CD3 and anti-CD28 mAbs, and the CD8$^+$ T cell blasts maintained for several days in IL-2-containing medium. No obvious increase of XBP-1s mRNA was detected during culture with IL-2 alone (Fig. 2*A* at 0 h and an additional 24-h culture without TCR ligation). In contrast, restimulation with anti-CD3 and anti-CD28 mAbs clearly induced splicing and XBP-1s accumulation in CD8$^+$ T cell blasts (Fig. 2*A*). This observation was also confirmed at the protein level by Western blot (Fig. 2*B*). We noted that XBP-1s gradually disappeared 8–24 h after TCR stimulation (Fig. 2, *A* and *B*). These results suggest that whereas IL-2 up-regulates XBP-1 transcripts, antigenic stimulation through the TCR is required for the generation of transcriptionally active XBP-1s.

Activation of the IRE-1/XBP-1 pathway in effector CD8$^+$ T cells during acute infection

Acute infection with viruses or bacteria induces vigorous expansion of Ag-specific CD8$^+$ T cells. We hypothesized that these dynamic CD8$^+$ T cell responses involving both inflammatory and antigenic stimuli would activate the IRE-1/XBP-1 pathway. After LCMV infection, most of the CD8$^+$ T cell population consists of LCMV-specific effector cells 8 days postinfection (p.i.) (36). Total CD8$^+$ T cells in the spleen of LCMV-infected C57BL/6J mice were examined

8 days p.i. for XBP-1 mRNA splicing. As shown in Fig. 3*A*, whereas $CD8^+$ T cells from uninfected mice contained no or little XBP-1s mRNA, LCMV infection clearly induced IRE-1-mediated splicing and generated XBP-1s mRNA in $CD8^+$ T cells.

To investigate XBP-1 splicing status in different subsets of effector $CD8^+$ T cells, we used transgenic mice that ubiquitously express an XBP-1 splicing reporter, referred to as ER stress-activated indicator, ERAI (28). In this system, Venus (a GFP variant) is expressed only in cells that contain XBP-1 splicing activity (Fig. 3*B*). Consistent with the previous report showing that dendritic cells constitutively activate the XBP-1 pathway (27), unstimulated splenic $CD11c^{high}$ dendritic cells from the ERAI transgenic mice were positive for Venus-GFP (Fig. 3*C*). Before infection, $CD8^+$ T cells from various organs of the ERAI mice showed no detectable signal of XBP-1 splicing activity (data not shown). However, gp_{33}-specific effector cells from LCMV-infected ERAI mice demonstrated XBP-1 splicing activity 8 days p.i. (Fig. 3*D*). When costained with KLRG1, the splicing activity was detectable in both $KLRG1^{low}$ and $KLRG1^{high}$ populations, but was significantly enriched in the $KLRG1^{high}$ terminal effector population (Fig. 3*E*).

Splicing of XBP-1u mRNA in effector $CD8^+$ T cells was also triggered during a bacterial infection with LM-OVA (Fig. 3, *F* and *G*). Similar to LCMV infection, the splicing activity was skewed to the $KLRG1^{high}$ population in effector $CD8^+$ T cells specific for OVA (Fig. 3*F*). Time-course analyses showed that XBP-1 mRNA splicing mainly occurred during primary expansion (~day 7 or 8 p.i.) and secondary expansion after rechallenge of Ag-specific $CD8^+$ T cells (Fig. 3, *F–H*). These results demonstrated that the IRE-1/XBP-1 splicing response is activated in effector $CD8^+$ T cells during acute infection, and suggest a correlation between high levels of XBP-1s and terminal differentiation of effector $CD8^+$ T cells.

Overexpression of XBP-1s enhances KLRG1 levels on effector $CD8^+$ T cells

Enrichment of the XBP-1 splicing activity in $KLRG1^{high}$ effector cells suggested that overexpression of XBP-1s would promote terminal differentiation. OT-I/$RAG1^{-/-}$ $CD8^+$ T cells were stimulated in vitro to allow retroviral transduction of various forms of XBP-1. Transduced OT-I/$RAG1^{-/-}$ cells, marked by Thy1.1 expression, were sorted and adoptively transferred (10^4 cells/mouse) into Thy1.1-negative host mice that were subsequently infected with 3000 CFU LM-OVA. After infection, XBP-1u, XBP-1s, and mock-transduced OT-I/$RAG1^{-/-}$ cells expanded and contracted with similar kinetics (Fig. 4, *A* and *B*). Cytokine expression in these OT-I/$RAG1^{-/-}$ effector cells at day 7 p.i. following 4 h of peptide stimulation was not significantly affected (data not shown). However, KLRG1 levels on XBP-1s transduced effector OT-I/$RAG1^{-/-}$ cells were clearly higher at day 7 p.i. than on mock-transduced cells, and the higher expression levels were maintained thereafter (Fig. 4*C*). XBP-1u overexpression had no such enhancing effect. Following *Listeria* infection, shortening the infectious period by antibiotic treatment hampers the terminal differentiation of effector $CD8^+$ T cells (4, 30). Accordingly, ampicillin treatment starting at 24 h p.i. diminished the differentiation of mock-transduced OT-I/$RAG1^{-/-}$ cells into the $KLRG1^{high}$ population, and this effect was reversed by retroviral expression of XBP-1s (Fig. 4*D*). In contrast to retroviral expression of T-bet, which is known to regulate effector $CD8^+$ T cell differentiation (4, 37), KLRG1 expression was not induced by XBP-1s expression itself during 10 days of in vitro culture with IL-2 (Fig. 4*E*). These results suggest that XBP-1s potentiates KLRG1 levels on effector $CD8^+$ T cells but does not directly control the expression.

Down-regulation of XBP-1 limits the development of $KLRG1^{high}$ effector $CD8^+$ T cells

We next tried to suppress XBP-1 levels by expressing a dominant negative form of XBP-1 (dnXBP-1) that possesses the DNA binding domain but lacks the transactivating domain (27, 34). Retro-viral-mediated expression of dnXBP-1 significantly suppressed KLRG1 levels on

transduced effector OT-I/RAG1$^{-/-}$ cells at day 7 after infection with LM-OVA (Fig. 5*A*). To further investigate the role of XBP-1 in CD8$^+$ T cells, we made use of XBP-1$^{-/-}$ cells from RAG2$^{-/-}$ blastocyst chimeras (38). Bone marrow chimeric mice containing XBP-1$^{-/-}$ CD8$^+$ T cells were generated using cells from XBP-1/RAG2$^{-/-}$ blastocyst chimeras (25,27). In these bone marrow chimeras, XBP-1$^{-/-}$ CD8$^+$ T cells were detected by the CD229.1 allelic marker, which is not expressed on host cells of C57BL/6 origin. Bone marrow cells from 129WT/RAG2$^{-/-}$ blastocyst chimeras were used to generate control bone marrow chimeras. These bone marrow chimeras were infected with LCMV, and effector CD8$^+$ T cell populations were examined 8 days later. Although similar levels of the gp_{33}-specific response were observed by WT and knockout cells, XBP-1$^{-/-}$ CD8$^+$ T cells formed a proportionally smaller KLRG1^{high}CD127^{low} population than did the WT cells (Fig. 5, *B* and *C*). The lack of XBP-1 did not severely impact cytokine production during a 4-h stimulation period (data not shown). These results suggest that XBP-1 is not required to mount a robust CD8$^+$ T cell response to acute infection, but is required for the optimal differentiation of effector CD8$^+$ T cells.

Discussion

In the present study, we demonstrated that the IRE-1/XBP-1 splicing machinery, known to be involved in the UPR, is activated in effector CD8$^+$ T cells during acute infection. IL-2 signals (as well as IL-4 and IL-15 in vitro) up-regulate XBP-1 mRNA in CD8$^+$ T cells in vivo, whereas TCR stimulation induces splicing and the generation of XBP-1s in vitro. Previous gene profiling studies showed that XBP-1 mRNA is up-regulated by IL-2 in vitro in human PBMC and mouse CD4$^+$ T cells (39–42), suggesting a common mechanism of XBP-1 induction in T cells. Furthermore, we showed that XBP-1s contributes to driving terminal differentiation of effector CD8$^+$ T cells. IRE-1 is an ER resident kinase/RNase that senses ER stress and is responsible for splicing XBP-1u mRNA (16,17). When the UPR is pharmacologically induced in human cell lines, IRE-1 activities are quickly attenuated, compared with the other two pathways of UPR (22). Interestingly, under persistent ER stress, cells survive longer when the IRE-1 RNase activity is artificially sustained (22). Thus, the IRE-1/XBP-1 pathway affects cell fate decisions between cytoprotective and proapoptotic outcomes by the UPR. We consistently observed that the level of XBP-1s waned 8–24 h after anti-CD3 and anti-CD28 mAb stimulation (Fig. 2), suggesting that CD8$^+$ T cells use a similar mechanism to turn this pathway off. Our gain-of-function and loss-of-function studies suggested a positive regulatory role for XBP-1s in KLRG1 expression. Unlike T-bet, however, overexpression of XBP-1s itself did not induce KLRG1 expression on CD8$^+$ T cells in vitro (Fig. 4*E*). In addition, XBP-1s did not significantly affect KLRG1 levels on responding CD8$^+$ T cells on day 5 following infection (Fig. 4*C*), when the cell fate commitment to terminal effectors vs memory precursor cells has already begun (4,5). It has been reported that KLRG1 expression is associated with extensive cell division (43). Therefore, we assume that XBP-1s supports, rather than directs, differentiation of CD8$^+$ T cells toward end-stage effector cells, possibly by affecting cell survival or proliferation.

The induction of XBP-1 mRNA and regulation of the unique splicing in CD8$^+$ T cells appeared analogous to that in B cells. XBP-1u mRNA is induced in B cells by IL-4, but splicing to XBP-1s mRNA requires further stimulation with LPS and/or CD40 engagement (26). XBP-1 has a nonredundant role in the differentiation of B cells into plasma cells (25,26), whereas one of the other arms of UPR, the PERK/eIF2α pathway, is not significantly involved in this process (44,45). Our DNA microarray data showed that ATF4 mRNA, which is downstream of the PERK/eIF2α pathway, is also up-regulated in CD8$^+$ T cells after IL-2 complex treatment (Table I). In future, it will be intriguing to examine the role of other pathways of the UPR in CD8$^+$ T cell responses.

Virus infection activates the UPR in host cells due to the massive production of viral proteins (46), raising the question of whether this is happening in our in vivo studies. LCMV can infect T cells, but at a very low rate (<1%), as judged by intracellular staining for LCMV nucleoprotein (47). Furthermore, splicing of XBP-1u mRNA was also evident in $CD8^+$ T cells after bacterial infection (Fig. 3, *F* and *G*). Therefore, it is not likely that the activation of XBP-1 splicing machinery in $CD8^+$ T cells is a consequence of direct infection. In vitro experiments demonstrating the splicing of XBP-1 mRNA after TCR ligation (Fig. 2) further reinforce this conclusion.

Does the activation of the XBP-1 splicing machinery in $CD8^+$ T cells represent induction of the UPR? Effector $CD8^+$ T cells produce many cytokines and cytotoxic molecules, and calcium release from the ER is induced upon TCR ligation, both of which potentially cause ER stress. However, a Gene Expression Omnibus database search (GSE10239 (5), and GSE9650 (48)) and our preliminary real-time PCR analyses (data not shown) revealed that UPR target genes such as Bip (*Hspa5*), CHOP (*Ddit3*), ERdj4 (*Dnajb9*), and EDEM (*Edem1*) were not significantly increased in $CD8^+$ T cells during the course of LCMV infection. Furthermore, in contrast to our expectation, cytokine production by $CD8^+$ T cells during a brief period of Ag stimulation in vitro was not changed by the forced expression of XBP-1s or a null mutation of XBP-1 (data not shown). XBP-1 may be required for the sustained production of these effector cytokines, similar to its role in μ chain production in B cells (49). UPR induction in the course of plasma cell differentiation is well documented (14,50). Despite the almost complete block of plasma cell differentiation in the absence of XBP-1 (25), however, Iwakoshi et al. (26) described that induction of ER chaperones including GRP78 (Bip) and GRP94 is only slightly impaired in XBP-$1^{-/-}$ B cells. Furthermore, Tirosh et al. (49) reported only a minor role for XBP-1 in ER quality control of primary B cells. ChIP-on-ChIp analysis of XBP-1 using different cell types identified a number of cell type- and condition-specific target genes (20). These observations suggest an as yet unknown role for XBP-1 beyond that in the UPR, which may be applicable to $CD8^+$ T cell responses. It is also possible that UPR target gene products are simply maintained at pre-existing levels by XBP-1s during the dramatic burst of proliferation of Ag-specific $CD8^+$ T cells responding to pathogen infection (1).

In summary, we have demonstrated the activation of IRE-1/XBP-1 splicing machinery in $CD8^+$ T cells in a physiological context. These findings also suggest that the stress control pathway in the ER contributes to the differentiation of effector $CD8^+$ T cells in vivo.

Acknowledgments

We thank Beverly Dere, Xiao-cun Pan, and Biswajit Paul for excellent technical support. We also thank Hao Shen for LM-OVA and LM-GP_{33}, Philippa Marrack for the pMit retrovirus vector, Masayuki Miura for ERAI transgenic mice and ERAI DNA constructs, and Laurie H. Glimcher for XBP-1/$RAG2^{-/-}$ blastocyst chimeras and the retroviral vector containing T-bet cDNA.

References

1. Blattman JN, Antia R, Sourdive DJ, Wang X, Kaech SM, Murali-Krishna K, Altman JD, Ahmed R. Estimating the precursor frequency of naive antigen-specific CD8 T cells. J Exp Med 2002;195:657–664. [PubMed: 11877489]
2. Williams MA, Bevan MJ. Effector and memory CTL differentiation. Annu Rev Immunol 2007;25:171–192. [PubMed: 17129182]
3. Kaech SM, Tan JT, Wherry EJ, Konieczny BT, Surh CD, Ahmed R. Selective expression of the interleukin 7 receptor identifies effector CD8 T cells that give rise to long-lived memory cells. Nat Immunol 2003;4:1191–1198. [PubMed: 14625547]

4. Joshi NS, Cui W, Chandele A, Lee HK, Urso DR, Hagman J, Gapin L, Kaech SM. Inflammation directs memory precursor and short-lived effector CD8$^+$ T cell fates via the graded expression of T-bet transcription factor. Immunity 2007;27:281–295. [PubMed: 17723218]
5. Sarkar S, Kalia V, Haining WN, Konieczny BT, Subramaniam S, Ahmed R. Functional and genomic profiling of effector CD8 T cell subsets with distinct memory fates. J Exp Med 2008;205:625–640. [PubMed: 18316415]
6. Blattman JN, Grayson JM, Wherry EJ, Kaech SM, Smith KA, Ahmed R. Therapeutic use of IL-2 to enhance antiviral T-cell responses in vivo. Nat Med 2003;9:540–547. [PubMed: 12692546]
7. D'Souza WN, Lefrancois L. IL-2 is not required for the initiation of CD8 T cell cycling but sustains expansion. J Immunol 2003;171:5727–5735. [PubMed: 14634080]
8. Williams MA, Tyznik AJ, Bevan MJ. Interleukin-2 signals during priming are required for secondary expansion of CD8$^+$ memory T cells. Nature 2006;441:890–893. [PubMed: 16778891]
9. Bachmann MF, Wolint P, Walton S, Schwarz K, Oxenius A. Differential role of IL-2R signaling for CD8$^+$ T cell responses in acute and chronic viral infections. Eur J Immunol 2007;37:1502–1512. [PubMed: 17492805]
10. Boyman O, Kovar M, Rubinstein MP, Surh CD, Sprent J. Selective stimulation of T cell subsets with antibody-cytokine immune complexes. Science 2006;311:1924–1927. [PubMed: 16484453]
11. Kamimura D, Sawa Y, Sato M, Agung E, Hirano T, Murakami M. IL-2 in vivo activities and antitumor efficacy enhanced by an anti-IL-2 mAb. J Immunol 2006;177:306–314. [PubMed: 16785526]
12. Kamimura D, Bevan MJ. Naive CD8$^+$ T cells differentiate into protective memory-like cells after IL-2 anti IL-2 complex treatment in vivo. J Exp Med 2007;204:1803–1812. [PubMed: 17664293]
13. Szegezdi E, Logue SE, Gorman AM, Samali A. Mediators of endoplasmic reticulum stress-induced apoptosis. EMBO Rep 2006;7:880–885. [PubMed: 16953201]
14. Wu J, Kaufman RJ. From acute ER stress to physiological roles of the unfolded protein response. Cell Death Differ 2006;13:374–384. [PubMed: 16397578]
15. Ron D, Walter P. Signal integration in the endoplasmic reticulum unfolded protein response. Nat Rev Mol Cell Biol 2007;8:519–529. [PubMed: 17565364]
16. Yoshida H, Matsui T, Yamamoto A, Okada T, Mori K. XBP1 mRNA is induced by ATF6 and spliced by IRE1 in response to ER stress to produce a highly active transcription factor. Cell 2001;107:881–891. [PubMed: 11779464]
17. Calfon M, Zeng H, Urano F, Till JH, Hubbard SR, Harding HP, Clark SG, Ron D. IRE1 couples endoplasmic reticulum load to secretory capacity by processing the XBP-1 mRNA. Nature 2002;415:92–96. [PubMed: 11780124]
18. Yoshida H, Oku M, Suzuki M, Mori K. pXBP1(U) encoded in XBP1 pre-mRNA negatively regulates unfolded protein response activator pXBP1(S) in mammalian ER stress response. J Cell Biol 2006;172:565–575. [PubMed: 16461360]
19. Lee AH, Iwakoshi NN, Glimcher LH. XBP-1 regulates a subset of endoplasmic reticulum resident chaperone genes in the unfolded protein response. Mol Cell Biol 2003;23:7448–7459. [PubMed: 14559994]
20. Acosta-Alvear D, Zhou Y, Blais A, Tsikitis M, Lents NH, Arias C, Lennon CJ, Kluger Y, Dynlacht BD. XBP1 controls diverse cell type- and condition-specific transcriptional regulatory networks. Mol Cell 2007;27:53–66. [PubMed: 17612490]
21. Rutkowski DT, Kaufman RJ. That which does not kill me makes me stronger: adapting to chronic ER stress. Trends Biochem Sci 2007;32:469–476. [PubMed: 17920280]
22. Lin JH, Li H, Yasumura D, Cohen HR, Zhang C, Panning B, Shokat KM, Lavail MM, Walter P. IRE1 signaling affects cell fate during the unfolded protein response. Science 2007;318:944–949. [PubMed: 17991856]
23. Reimold AM, Etkin A, Clauss I, Perkins A, Friend DS, Zhang J, Horton HF, Scott A, Orkin SH, Byrne MC, et al. An essential role in liver development for transcription factor XBP-1. Genes Dev 2000;14:152–157. [PubMed: 10652269]
24. Lee AH, Chu GC, Iwakoshi NN, Glimcher LH. XBP-1 is required for biogenesis of cellular secretory machinery of exocrine glands. EMBO J 2005;24:4368–4380. [PubMed: 16362047]

25. Reimold AM, Iwakoshi NN, Manis J, Vallabhajosyula P, Szomolanyi-Tsuda E, Gravallese EM, Friend D, Grusby MJ, Alt F, Glimcher LH. Plasma cell differentiation requires the transcription factor XBP-1. Nature 2001;412:300–307. [PubMed: 11460154]
26. Iwakoshi NN, Lee AH, Vallabhajosyula P, Otipoby KL, Rajewsky K, Glimcher LH. Plasma cell differentiation and the unfolded protein response intersect at the transcription factor XBP-1. Nat Immunol 2003;4:321–329. [PubMed: 12612580]
27. Iwakoshi NN, Pypaert M, Glimcher LH. The transcription factor XBP-1 is essential for the development and survival of dendritic cells. J Exp Med 2007;204:2267–2275. [PubMed: 17875675]
28. Iwawaki T, Akai R, Kohno K, Miura M. A transgenic mouse model for monitoring endoplasmic reticulum stress. Nat Med 2004;10:98–102. [PubMed: 14702639]
29. Pope C, Kim SK, Marzo A, Masopust D, Williams K, Jiang J, Shen H, Lefrancois L. Organ-specific regulation of the CD8 T cell response to *Listeria monocytogenes* infection. J Immunol 2001;166:3402–3409. [PubMed: 11207297]
30. Williams MA, Bevan MJ. Shortening the infectious period does not alter expansion of CD8 T cells but diminishes their capacity to differentiate into memory cells. J Immunol 2004;173:6694–6702. [PubMed: 15557161]
31. Tardif KD, Mori K, Kaufman RJ, Siddiqui A. Hepatitis C virus suppresses the IRE1-XBP1 pathway of the unfolded protein response. J Biol Chem 2004;279:17158–17164. [PubMed: 14960590]
32. Mitchell TC, Hildeman D, Kedl RM, Teague TK, Schaefer BC, White J, Zhu Y, Kappler J, Marrack P. Immunological adjuvants promote activated T cell survival via induction of Bcl-3. Nat Immunol 2001;2:397–402. [PubMed: 11323692]
33. Ouyang W, Ranganath SH, Weindel K, Bhattacharya D, Murphy TL, Sha WC, Murphy KM. Inhibition of Th1 development mediated by GATA-3 through an IL-4-independent mechanism. Immunity 1998;9:745–755. [PubMed: 9846495]
34. Lee AH, Iwakoshi NN, Anderson KC, Glimcher LH. Proteasome inhibitors disrupt the unfolded protein response in myeloma cells. Proc Natl Acad Sci USA 2003;100:9946–9951. [PubMed: 12902539]
35. Yun TJ, Bevan MJ. Notch-regulated ankyrin-repeat protein inhibits Notch1 signaling: multiple Notch1 signaling pathways involved in T cell development. J Immunol 2003;170:5834–5841. [PubMed: 12794108]
36. Masopust D, Murali-Krishna K, Ahmed R. Quantitating the magnitude of the lymphocytic choriomeningitis virus-specific CD8 T-cell response: it is even bigger than we thought. J Virol 2007;81:2002–2011. [PubMed: 17151096]
37. Intlekofer AM, Takemoto N, Kao C, Banerjee A, Schambach F, Northrop JK, Shen H, Wherry EJ, Reiner SL. Requirement for T-bet in the aberrant differentiation of unhelped memory $CD8^+$ T cells. J Exp Med 2007;204:2015–2021. [PubMed: 17698591]
38. Chen J, Lansford R, Stewart V, Young F, Alt FW. RAG-2-deficient blastocyst complementation: an assay of gene function in lymphocyte development. Proc Natl Acad Sci USA 1993;90:4528–4532. [PubMed: 8506294]
39. Beadling C, Smith KA. DNA array analysis of interleukin-2-regulated immediate/early genes. Med Immunol 2002;1:2. [PubMed: 12459040]
40. Kovanen PE, Rosenwald A, Fu J, Hurt EM, Lam LT, Giltnane JM, Wright G, Staudt LM, Leonard WJ. Analysis of γ_c-family cytokine target genes: identification of dual-specificity phosphatase 5 (DUSP5) as a regulator of mitogen-activated protein kinase activity in interleukin-2 signaling. J Biol Chem 2003;278:5205–5213. [PubMed: 12435740]
41. Bensinger SJ, Walsh PT, Zhang J, Carroll M, Parsons R, Rathmell JC, Thompson CB, Burchill MA, Farrar MA, Turka LA. Distinct IL-2 receptor signaling pattern in $CD4^+CD25^+$ regulatory T cells. J Immunol 2004;172:5287–5296. [PubMed: 15100267]
42. Kovanen PE, Young L, Al-Shami A, Rovella V, Pise-Masison CA, Radonovich MF, Powell J, Fu J, Brady JN, Munson PJ, Leonard WJ. Global analysis of IL-2 target genes: identification of chromosomal clusters of expressed genes. Int Immunol 2005;17:1009–1021. [PubMed: 15980098]
43. Voehringer D, Blaser C, Brawand P, Raulet DH, Hanke T, Pircher H. Viral infections induce abundant numbers of senescent CD8 T cells. J Immunol 2001;167:4838–4843. [PubMed: 11673487]

44. Zhang K, Wong HN, Song B, Miller CN, Scheuner D, Kaufman RJ. The unfolded protein response sensor IRE1α is required at 2 distinct steps in B cell lymphopoiesis. J Clin Invest 2005;115:268–281. [PubMed: 15690081]

45. Gass JN, Jiang HY, Wek RC, Brewer JW. The unfolded protein response of B-lymphocytes: PERK-independent development of antibody-secreting cells. Mol Immunol 2008;45:1035–1043. [PubMed: 17822768]

46. He B. Viruses, endoplasmic reticulum stress, and interferon responses. Cell Death Differ 2006;13:393–403. [PubMed: 16397582]

47. Sevilla N, Kunz S, Holz A, Lewicki H, Homann D, Yamada H, Campbell KP, de La Torre JC, Oldstone MB. Immunosuppression and resultant viral persistence by specific viral targeting of dendritic cells. J Exp Med 2000;192:1249–1260. [PubMed: 11067874]

48. Wherry EJ, Ha SJ, Kaech SM, Haining WN, Sarkar S, Kalia V, Subramaniam S, Blattman JN, Barber DL, Ahmed R. Molecular signature of $CD8^+$ T cell exhaustion during chronic viral infection. Immunity 2007;27:670–684. [PubMed: 17950003]

49. Tirosh B, Iwakoshi NN, Glimcher LH, Ploegh HL. XBP-1 specifically promotes IgM synthesis and secretion, but is dispensable for degradation of glycoproteins in primary B cells. J Exp Med 2005;202:505–516. [PubMed: 16103408]

50. Gass JN, Gunn KE, Sriburi R, Brewer JW. Stressed-out B cells? Plasma-cell differentiation and the unfolded protein response. Trends Immunol 2004;25:17–24. [PubMed: 14698280]

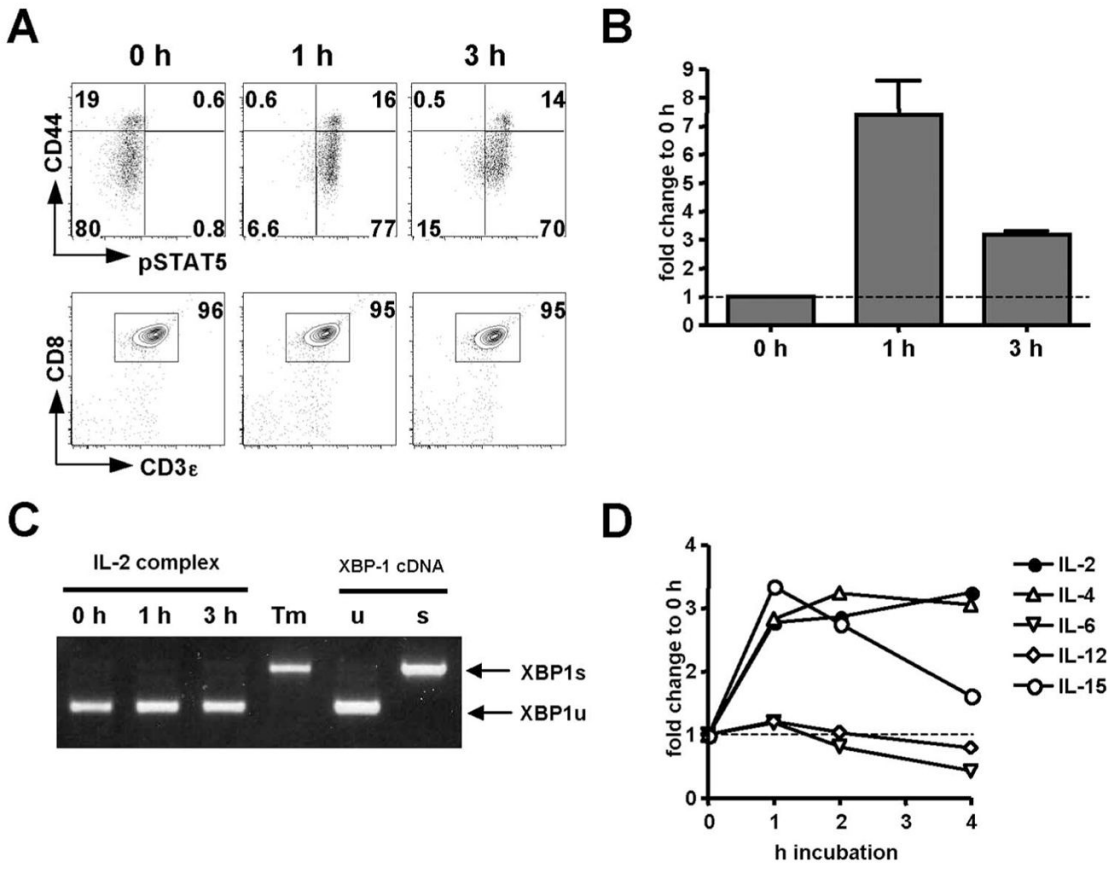

FIGURE 1.

XBP-1u mRNA is up-regulated in $CD8^+$ T cells following IL-2 complex treatment in vivo. *A*, STAT5 phosphorylation of $CD8^+$ T cells after IL-2 complex injection (*top row*) and purity of the sorted samples for DNA microarray analysis (*bottom row*). *B*, Up-regulation of total XBP-1 mRNA in $CD8^+$ T cells after IL-2 complex treatment assayed by real-time PCR. Data represent the mean ± SEM ($n = 2$ experiments). *C*, Splicing status of XBP-1 mRNA detected by RT-PCR plus *Pst*I digestion. cDNA from a mouse melanoma cell line treated with tunicamycin (Tm) for 6 h, and XBP-1u and XBP-1s cDNA were used as control templates for this assay. *D*, OT-I/RAG1$^{-/-}$ $CD8^+$ T cell blasts that had been rested overnight without IL-2 were stimulated with cytokines (10 ng/ml) for the indicated periods before real-time PCR was performed for total XBP-1 mRNA.

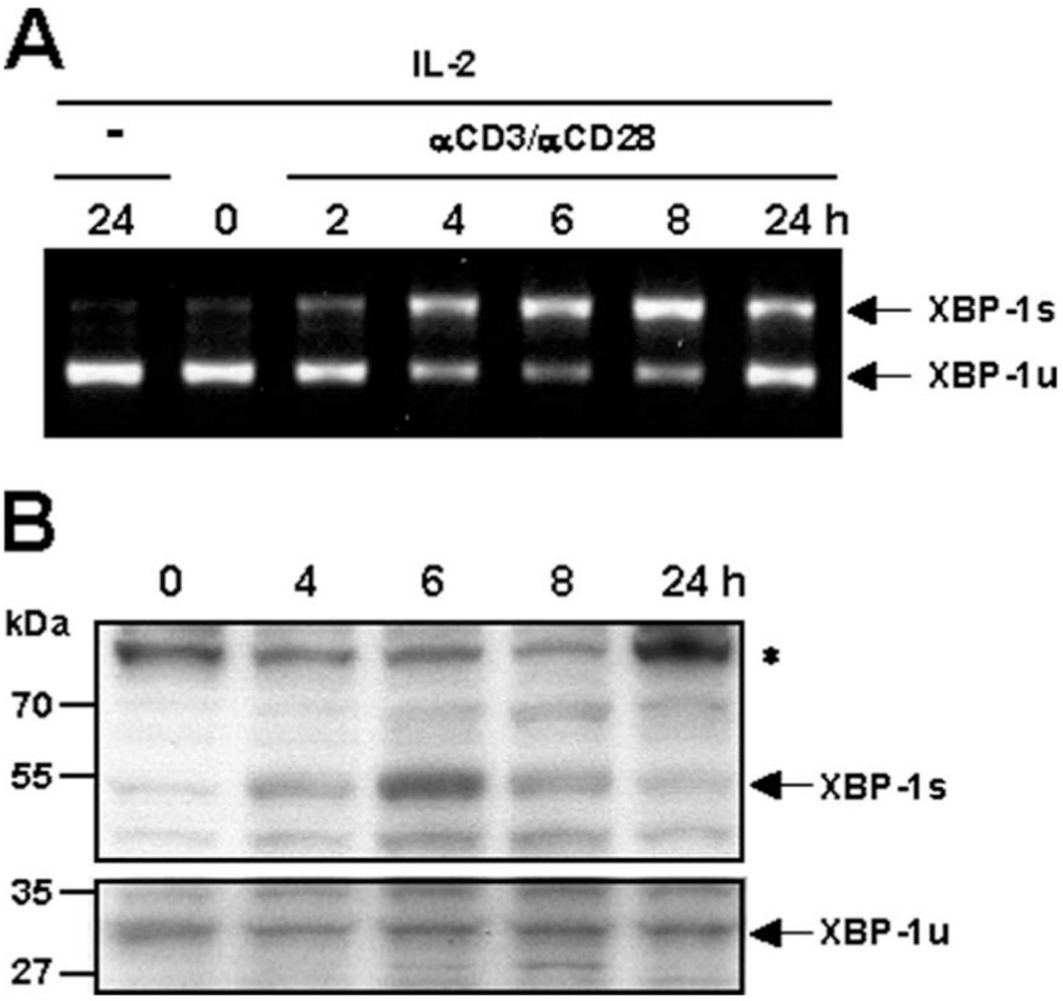

FIGURE 2.

TCR stimulation induces splicing of XBP-1 message. Purified $CD8^+$ T cells were activated with plate-bound anti-CD3 and anti-CD28 mAbs, and maintained in IL-2-containing medium. These $CD8^+$ T cell blasts were restimulated with anti-CD3 and anti-CD28 mAbs for the indicated times. *A*, Splicing of XBP-1u mRNA detected by RT-PCR and *Pst*I digestion. *B*, Western blot analysis detecting both forms of XBP-1. A nonspecific band as a loading control is indicated (*).

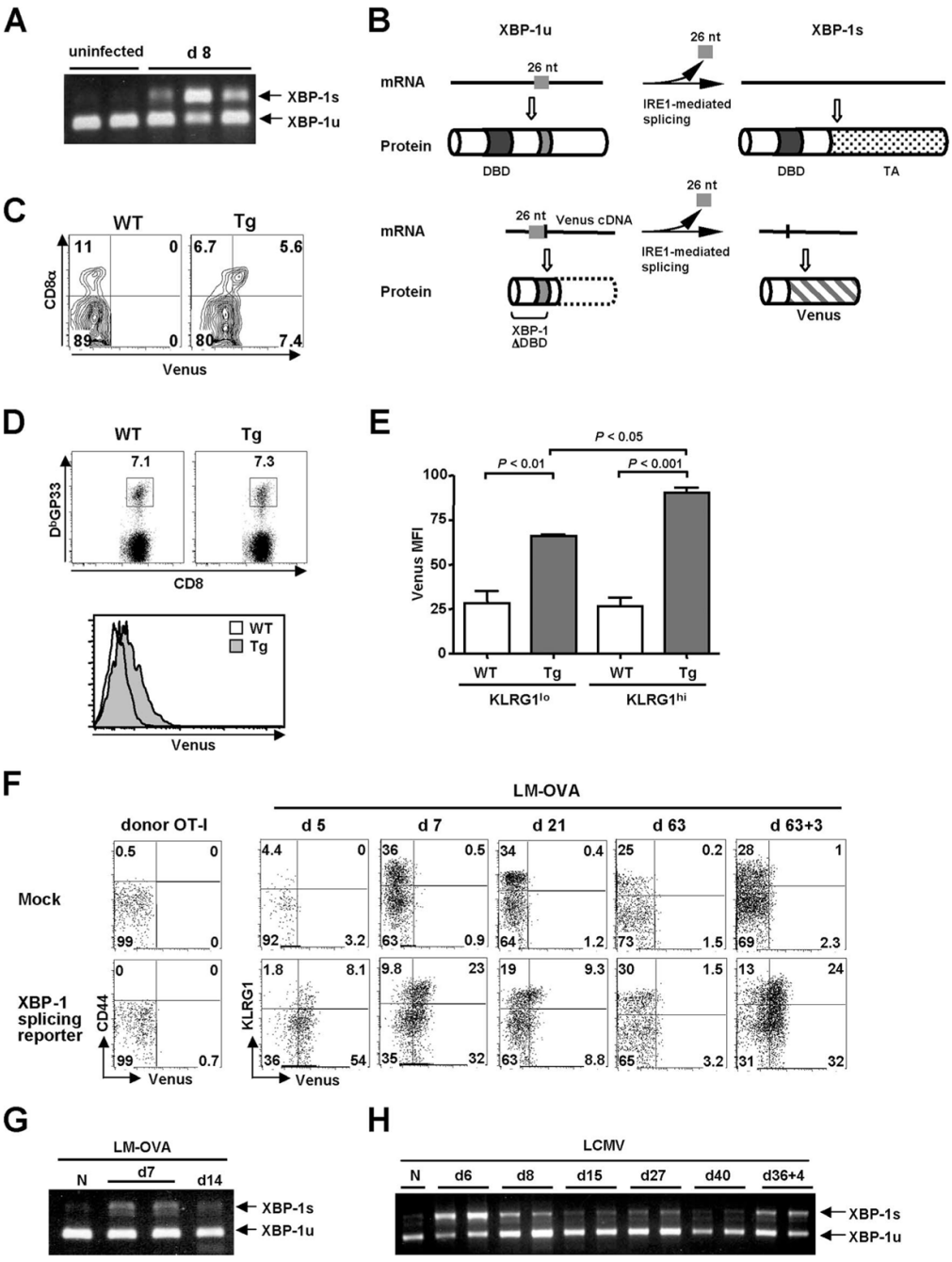

FIGURE 3.

Acute infection activates the IRE-1/XBP-1 pathway in $CD8^+$ T cells. *A*, Splicing status of XBP-1 mRNA in total $CD8^+$ T cells purified from uninfected or LCMV-infected mice at day 8 p.i. Each lane represents an individual animal. *B*, The XBP-1-splicing reporter system. After removal of the 26-nt intron, the Venus-GFP cDNA becomes in-frame in the reporter construct. The reporter construct lacks the DNA binding domain (DBD) to prevent a dominant negative action of the truncated XBP-1 protein (28). TA, transcriptional activating domain. *C*, Venus-GFP levels in splenic dendritic cells of ERAI transgenic mice. Plots are gated on $CD3\varepsilon^-CD19^-CD11c^{high}$ population. *D*, WT and ERAI transgenic (Tg) reporter mice were infected with LCMV, and splenocytes stained with D^b gp_{33} tetramer on day 8. Plots are gated

on $CD8^+$ cells. The percentage of gp_{33}-specific population within $CD8^+$ cells (*top*) is shown. Venus-GFP levels in gated gp_{33}-specific $CD8^+$ T cells (*bottom*) are shown. *E*, Mean fluorescence intensity (MFI) of Venus-GFP within $KLRG1^{low}$ or $KLRG1^{high}$ gp_{33}-specific $CD8^+$ T cell populations at day 8 p.i. Results indicate the mean ± SEM (n = 3–4 mice). *F*, OT-I cells expressing the XBP-1 splicing reporter or mock construct were obtained from mice reconstituted with retrovirally transduced bone marrow cells. These OT-I cells were transferred to host mice that were subsequently infected with 3000 CFU LM-OVA. Some infected animals were rested for 63 days, then given a high dose (1×10^5 CFU) of LM-OVA, and analyzed 3 days later (d63+3). Plots are gated on OT-I cells with Thy1.1 transduction marker. The percentage of the gated OT-1 cells within each quadrant is shown. *G*, Splicing status of XBP-1 mRNA in naive $CD44^{low}$ OT-I cells (N) or OT-I cells from mice that had received 10^4 naive OT-I cells and were then infected with LM-OVA. *H*, Splicing status of XBP-1 mRNA in naive $CD44^{low}$ P14 cells (N) or P14 cells from LCMV-infected mice that had received 10^4 naive P14 cells. Some previously infected mice were challenged with 2×10^5 CFU of LM-GP_{33}, and analyzed after 4 days (d36+4).

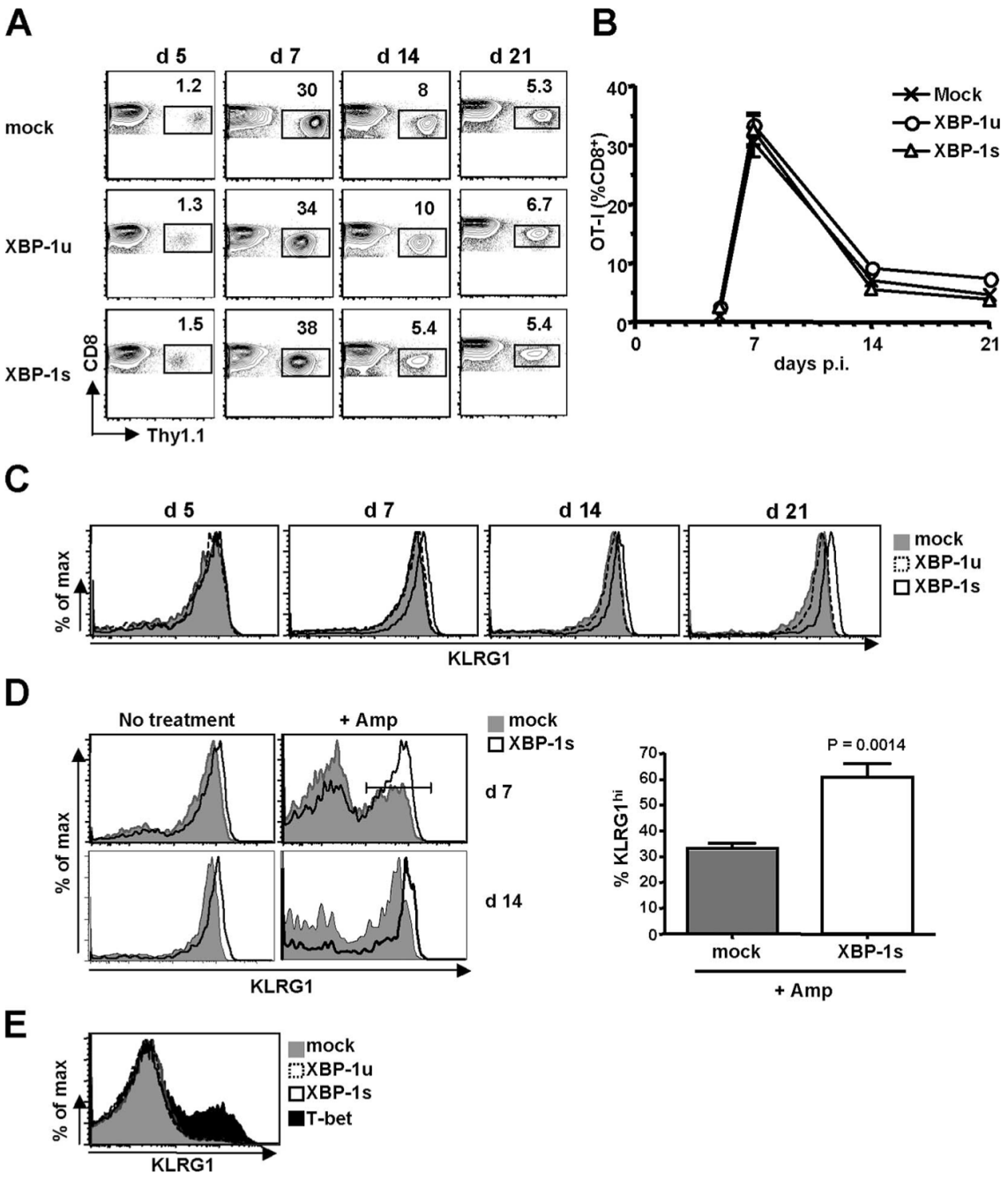

FIGURE 4.

Overexpression of XBP-1s enhances KLRG1 expression on effector CD8$^+$ T cells. *A*, OT-I/RAG1$^{-/-}$ cells transduced with retrovirus encoding XBP-1u or XBP-1s were sorted based on the expression of Thy1.1 transduction marker, and 10^4 cells were transferred to host mice that were subsequently infected with 3000 CFU of LM-OVA. Populations of transduced OT-I/RAG1$^{-/-}$ cells (Thy1.1$^+$) in the peripheral blood after infection are shown. Data are gated on CD8$^+$ cells. The percentage of transduced OT-I/RAG1$^{-/-}$ cells within the CD8$^+$ population is shown. *B*, Graphic representation of *A* with the mean ± SEM for n = 8–16 mice. *C*, KLRG1 levels on transduced OT-I/RAG$^{-/-}$ cells following LM-OVA infection. *D*, LM-OVA-infected mice containing mock- or XBP-1s-transduced OT-I/RAG$^{-/-}$ cells were treated with ampicillin,

starting at 24 h p.i. KLRG1 levels of OT-I/RAG1$^{-/-}$ cells are shown. The percentage of KLRG1^{high} population in OT-I/RAG$^{-/-}$ cells with ampicillin treatment on day 7, p.i. with the mean ± SEM for n = 4–5 mice. *E*, KLRG1 levels of OT-I/RAG1$^{-/-}$ cells transduced with XBP-1u, XBP-1s, or T-bet and cultured in vitro for 10 days.

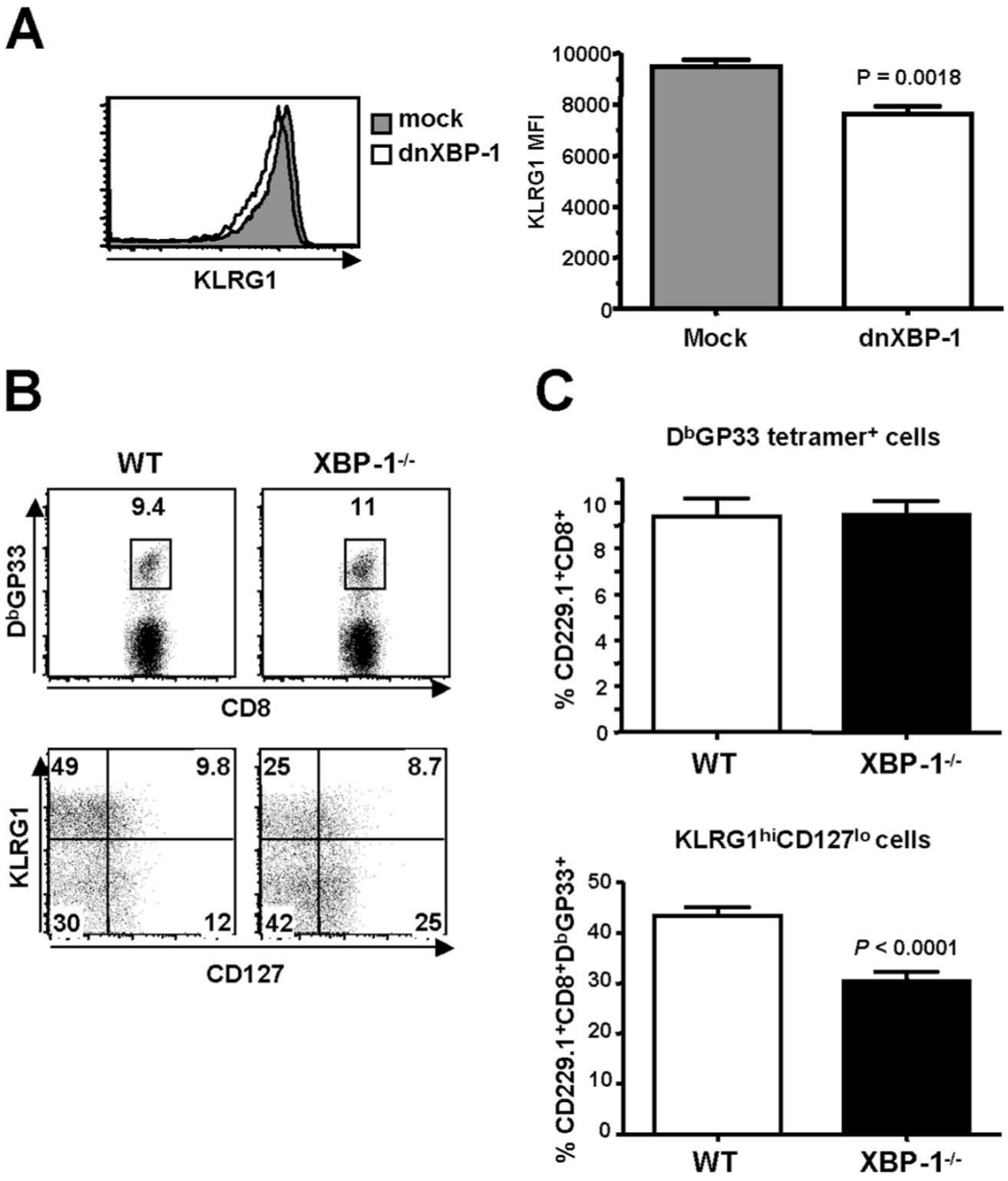

FIGURE 5.

Loss-of-function of XBP-1 results in diminished KLRG1^{high} effector CD8$^+$ T cell population. *A*, OT-I/RAG1$^{-/-}$ CD8$^+$ T cells were transduced with a dominant negative form of XBP-1 (dnXBP-1) and transferred to host mice, followed by infection with LM-OVA. KLRG1 levels on the transduced cells (day 7 p.i.) in the blood are shown. Graphic representation of mean fluorescence intensity (MFI) of KLRG1 (*right*). Results indicate the mean ± SEM (n = 5 mice each). *B*, WT or XBP-1$^{-/-}$ bone marrow chimeric mice were infected with LCMV. On day 8, gp_{33}-specific CD8$^+$ T cells in the blood were detected by tetramer staining. Percentage of D^bgp_{33} tetramer-positive within the donor CD8$^+$ population (*top*) gated on CD229.1$^+$ donor bone marrow-derived CD8$^+$ cells is shown. KLRG1 and CD127 levels on gp_{33}-specific CD8$^+$ T cells are shown. The percentage within the donor gp_{33}-specific CD8$^+$ T cells (*bottom*) is indicated. *C*, Graphic representation of data in *B* with the mean ± SEM for n = 8–10 mice.

Table I

Genes induced in $CD8^+$ T cells by IL-2 complex treatment

1 h/0 h[a]	3 h/0 h	Gene Title	Gene Symbol
5.5	5.4	Lymphotoxin A	*Lta*
5.3	4.3	Regulator of G protein signaling 1	*Rgs1*
5.1	4.7	Cytokine inducible Src homology 2-containing protein	*Cish*
4.4	4.1	MAPK kinase kinase 8	*Map3k8*
3.5	3.0	X-box-binding protein-1	*Xbp1*
3.3	3.1	B cell leukemia/lymphoma 2	*Bcl2*
3.2	1.6	Early growth response 1	*Egr1*
3.0	2.2	AXIN1 up-regulated 1	*Axud1*
2.8	2.8	CD69	*Cd69*
2.7	2.9	Suppressor of cytokine signaling 1	*Socs1*
2.7	1.7	Signaling lymphocytic activation molecule family member 1	*Slamf1*
2.6	2.1	A disintegrin and metallopeptidase domain 19	*Adam19*
2.4	2.9	Activating transcription factor 4	*Atf4*
2.3	1.8	Myelocytomatosis oncogene	*Myc*
2.2	1.2	FBJ osteosarcoma oncogene	*Fos*
2.2	2.0	Jun oncogene	*Jun*
2.1	2.4	Secreted frizzled-related protein 2	*Sfrp2*
2.1	−0.5	cDNA sequence BC023892	*BC023892*
2.1	1.4	Kruppel-like factor 6	*Klf6*
2.1	1.6	RAS p21 protein activator 2	*Rasa2*
2.0	2.5	Solute carrier family 30, member 4	*Slc30a4*
2.0	1.4	NF of κ light polypeptide gene enhancer in B cell inhibitor, ζ	*Nfkbiz*

[a] Fold change relative to 0 h is shown as a $\log_2$ value.

Table II

Genes repressed in $CD8^+$ T cells by IL-2 complex treatment

1 h/0 h[a]	3 h/0 h	Gene Title	Gene Symbol
−3.4	−1.5	Similar to mouse RING finger 1	*LOC630539*
−2.9	−1.8	Sestrin 1	*Sesn1*
−2.4	−1.1	Phosphodiesterase 4B, cAMP specific	*Pde4b*
−2.3	−1.9	Structural maintenance of chromosomes 4	*Smc4*
−2.2	−1.3	Sex comb on midleg-like 4 (Drosophila)	*Scml4*
−2.1	−2.2	RIKEN cDNA 4930431B09 gene	*4930431B09Rik*
−2.0	−1.9	Chemokine (C-X-C motif) receptor 4	*Cxcr4*
−2.0	−1.6	Kruppel-like factor 3 (basic)	*Klf3*
−2.0	−1.7	CD28	*Cd28*
−2.0	−1.6	Serum/glucocorticoid regulated kinase	*Sgk*
−2.0	−0.9	CXXC finger 5	*Cxxc5*
−2.0	−2.0	S100 calcium binding protein A10 (calpactin)	*S100a10*

[a] Fold change relative to 0 h (no treatment) is shown as a $\log_2$ value.